

MORE PIECES OF THE PUZZLE: CHEMISTRY AND SUBSTRUCTURES IN THE GALACTIC THICK DISK

AMINA HELMI¹, MARY WILLIAMS², K. C. FREEMAN³, J. BLAND-HAWTHORN⁴, AND G. DE SILVA⁵

¹ Kapteyn Astronomical Institute, University of Groningen, P.O. Box 800, 9700 AV Groningen, The Netherlands; ahelmi@astro.rug.nl

² Astrophysikalisches Institut Potsdam, An der Sternwarte 16, D-14482 Germany; mary@aip.de

³ Research School of Astronomy and Astrophysics The Australian National University, Cotter Road Weston Creek, ACT 2611, Australia

⁴ Sydney Institute for Astronomy, School of Physics A28, University of Sydney, NSW 2006, Australia

⁵ Australian Astronomical Observatory, P.O. Box 915, North Ryde, NSW 1670, Australia

Received 2014 January 8; accepted 2014 July 9; published 2014 August 6

ABSTRACT

We present a study of the chemical abundances of solar neighborhood stars associated with dynamical structures in the Milky Way’s (thick) disk. These stars were identified as an overdensity in the eccentricity range $0.3 < \epsilon < 0.5$ in the Copenhagen–Geneva Survey by Helmi et al. We find that stars with these dynamical characteristics do not constitute a homogeneous population. A relatively sharp transition in dynamical and chemical properties appears to occur at a metallicity of $[\text{Fe}/\text{H}] \sim -0.4$. Stars with $[\text{Fe}/\text{H}] > -0.4$ have mostly lower eccentricities, smaller vertical velocity dispersions, are α -enhanced, and define a rather narrow sequence in $[\alpha/\text{Fe}]$ versus $[\text{Fe}/\text{H}]$, clearly distinct from that of the thin disk. Stars with $[\text{Fe}/\text{H}] < -0.4$ have a range of eccentricities, are hotter vertically, and depict a larger spread in $[\alpha/\text{Fe}]$. We also found tentative evidence of a substructure possibly associated with the disruption of a metal-rich star cluster. The differences between these populations of stars is also present in, e.g., $[\text{Zn}/\text{Fe}]$, $[\text{Ni}/\text{Fe}]$, and $[\text{SmII}/\text{Fe}]$, suggesting a real physical distinction.

Key words: Galaxy: disk – Galaxy: formation – stars: abundances

Online-only material: color figures

1. INTRODUCTION

In the concordance Λ CDM cosmological model, mergers are ubiquitous and expected to have left imprints in galaxies like the Milky Way (Helmi & White 1999; Bullock & Johnston 2005). Although the majority of stars in disks have probably formed in situ, some fraction may have originated in accreted objects on low-inclination orbits (e.g., Abadi et al. 2003). Some evidence of such events may be the Monoceros ring in the outskirts of our Galaxy (Newberg et al. 2002, although its origin is still debated), the low-latitude substructures in M31 (Richardson et al. 2008), the Arcturus stream (Navarro et al. 2004), the ω Cen stream (Meza et al. 2005; Majewski et al. 2012), and the groups found by Helmi et al. (2006, hereafter H06) and Arifyanto & Fuchs (2006) near the Sun.

The recovery of such events is the focus of many surveys, and, correspondingly, attention has been given to the optimal search techniques. Most of the substructures discovered thus far have been identified in projections of phase-space, namely, spatial (e.g., Belokurov et al. 2006), kinematical (Gilmore et al. 2002), or in an “integrals of motion” space (Helmi et al. 1999). However, there is the intriguing suggestion that merger debris may also be identifiable through peculiar chemical abundance patterns (Freeman & Bland-Hawthorn 2002; De Silva et al. 2007), as stars that formed in a common system must have experienced similar star formation and enrichment histories. Some first detections of chemically peculiar sequences or clustering have been reported by Nissen & Schuster (2010, 2011) and Wylie-de Boer et al. (2010, 2012).

In this paper we present chemical abundances for a sample of nearby stars from the Copenhagen–Geneva survey found to define an overdensity in the eccentricity range $0.3 \leq \epsilon \leq 0.5$ by H06. We performed a high-resolution follow-up study of 72 of these stars, and supplemented this data set with that of Stonkute et al. (2012, 2013, hereafter ST) of 21 stars in the same overdensity. As we shall see below, a few subpopulations

of stars with different dynamics and chemical abundances co-exist in this region of Galactic (extended) phase-space.

2. OBSERVATIONS AND ANALYSIS

2.1. The Puzzle Stars

The stars in H06 were identified in the Copenhagen–Geneva survey (Nordström et al. 2004, GCS hereafter) because of their peculiar distribution in the space of orbital apocenter–pericenter and z -component of the angular momentum. These stars share similar relatively planar orbits with moderate eccentricities between 0.3 and 0.5. This eccentricity region is overdense with respect to what is expected for a smooth model of the Galaxy (see Figures 10, 11, and 13 of H06). Besides their characteristic dynamics, the 274 stars identified were found to have distinct metallicity and age distributions. A separation into three different groups based on their metallicity was proposed, namely, G1: $-0.45 < [\text{Fe}/\text{H}] < -0.2$ dex, G2: $([\text{Fe}/\text{H}] \sim -0.6$ dex, and G3: $[\text{Fe}/\text{H}] < -0.7$ dex, whereas the metallicity decreases, there is a tendency for the groups to have a larger mean eccentricity. Group G2 has some overlap with the Arcturus stream, in terms of its average V velocity and mean $[\text{Fe}/\text{H}]$. Note that these $[\text{Fe}/\text{H}]$ were estimated from Strömgren photometry and are slightly different from those derived here.

Figure 1 shows the velocity distribution of the revised GCS (Holmberg et al. 2009) highlighting the H06 stars. The stars included in this paper are indicated with solid symbols (those we followed-up with high-resolution spectroscopy), or with crosses (those from ST).

2.2. Derivation of Chemical Abundances

We performed our high signal-to-noise high-resolution spectroscopic study using UCLES on the 4 m Anglo Australian Telescope. It includes 36 members of G1 (27.5% of all candidates identified by H06), 22 members of G2 (25.6%), and 14

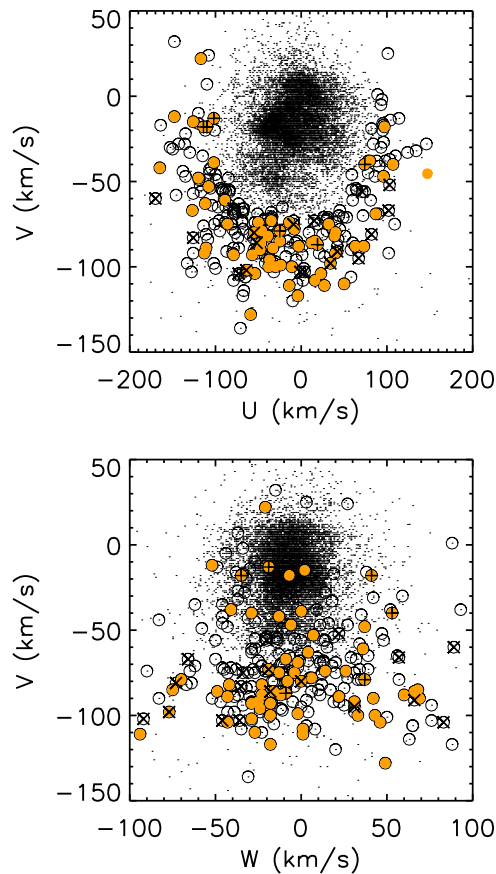


Figure 1. Velocities of stars in the revised **GCS** catalog, highlighting those from **H06**. The solid symbols correspond to those we followed-up with high-resolution spectroscopy, while the crosses are from **ST**. We kept only stars with revised eccentricities $0.275 \leq \epsilon \leq 0.525$. The stars with “+” symbols are those in the “tentative” cluster (see the main text).

(A color version of this figure is available in the online journal.)

members of G3 (20.6%). The wavelength coverage for our observations was 3850–5300 Å and at least three exposures of, on average, 400 s were done per star at a resolution $R \sim 45,000$. A signal-to-noise ratio of ~ 100 –150 per pixel at the central wavelength was obtained. The data were reduced using the standard IRAF routines *ccdred* and *echelle*, which included bias subtraction, flat-fielding, order extraction, scattered light subtraction, and wavelength calibration. We focus here on those stars with $(V - K) > 1.4$. Furthermore, two stars in G1 have significantly different eccentricities in the revised **GCS**, so we do not consider these further. We are thus left with a total of 64 stars: 30 from G1, 21 from G2, and 13 from G3.

To supplement this sample we also consider the 21 stars originally in G3 followed-up by **ST**. Two of these have also been observed by us, and three have significantly revised **GCS** eccentricities which place them outside of the region of interest. We are therefore left with 16 independent stars from this sample.

Elemental abundances were derived for our stars by performing a local thermodynamic equilibrium analysis with the MOOG code (Snedden 1973). To measure equivalent widths we used a modified version of the DAOSPEC program which automatically fits Gaussian profiles to lines in a spectrum (Stetson & Pancino 2008). The modifications involved disabling DAOSPEC’s continuum fitting, and instead performing hand-fitting for our crowded blue data. In this paper we present the abundances for our stars using stellar parameters calculated

using a “spectroscopic” (rather than physical) approach as they yielded better agreement for stars in common with external studies by Reddy et al. (2003, 2006) and Bensby et al. (2003, 2005). In this approach we force excitation and ionization balance to derive T_{eff} and $\log g$, respectively. Microturbulence is found by requiring that there be no dependence of abundance on line strength. We present here the abundance results for Mg, Ca, Ti, Cr, Ni, Zn, Nd, and Sm, using elements or lines for which hyperfine and isotopic splitting need not be considered. The first three elements represent the α elements (where $[\alpha/\text{Fe}] = [(\text{Mg}+\text{Ca}+\text{Ti})/3\text{Fe}]$); Cr, Ni, Zn represent Fe-peak elements; and Nd and Sm have a varying mix of *s*- and *r*-process contributions (Arlandini et al. 1999; Burris et al. 2000).

2.3. Results

We take a fresh look here at the **H06** stars now supplemented by the chemical abundances, rather than follow the originally proposed separation into groups.

The central panel of Figure 2 shows the distribution of orbital eccentricity ϵ for the **H06** stars as a function of $[\text{Fe}/\text{H}]$. Note that there appears to be a lack of stars in the upper right quadrant, i.e., for $\epsilon > 0.4$ at $[\text{Fe}/\text{H}] > -0.4$ (also the case in the full **H06** sample). This is also evident in the uppermost panel where we compare the $[\text{Fe}/\text{H}]$ cumulative distribution for the full sample (solid line), for stars with $\epsilon > 0.4$ (dashed line), and for those with $\epsilon < 0.4$ (dotted-dashed line). The probability that the latter two are drawn from the same parent metallicity distribution is 1.1×10^{-2} , according to a K-S test. On the other hand, the cumulative distribution of ϵ is plotted in the rightmost panel of the figure. The probability that the stars with $[\text{Fe}/\text{H}] < -0.4$ (dotted-dashed) and those with $[\text{Fe}/\text{H}] > -0.4$ dex (dashed) have the same eccentricity distribution is 4.7×10^{-4} according to a K-S test. Also intriguing is that the stars with $[\text{Fe}/\text{H}] < -0.4$ dex have on average a larger vertical velocity dispersion (47.7 km s^{-1}) compared to the group with high metallicity ($\sigma_z \sim 31.4 \text{ km s}^{-1}$).

The bottom panel of Figure 2 shows $[\alpha/\text{Fe}]$ versus $[\text{Fe}/\text{H}]$ for the stars in our sample, where the black solid symbols indicate those that we have followed-up and the crosses are those from **ST**. We have highlighted with open symbols a set of six stars with $[\text{Fe}/\text{H}] \sim -0.35$ dex. Closer examination of these stars reveals that three of them define a very cold kinematic group (visible in Figure 1 at $V \sim -15$ and $U \sim -100 \text{ km s}^{-1}$; + symbols). These stars’ eccentricities are 0.28, 0.31, and 0.32 while their $[\text{Fe}/\text{H}] = -0.36, -0.26,$ and -0.33 dex. The ϵ and $[\text{Fe}/\text{H}]$ of the remaining three stars are also similar as shown in the central panel of Figure 2. This is also true for the chemical abundances of these stars (Figure 4 below) for all measured elements except for $[\text{Mg}/\text{Fe}]$ (where even those stars in the kinematic group depict a larger spread).

There are two possible interpretations that we may put forward: (1) that the other three stars with similar $[\text{Fe}/\text{H}]$ are a random sample of the thin disk, whose orbits are slightly hotter than typical for this component; and (2) that they are part of the “kinematic clump” of three stars (a disrupted cluster?) because they are not very different dynamically, they have similar $[\text{Fe}/\text{H}]$ and other abundances, as well as being indistinguishable in age (and clearly younger than the upper $[\alpha/\text{Fe}]$ sequence at this metallicity). This is evident from Figure 3, where we plot the H-R diagram of the stars in our sample. The lines correspond to 7 (solid) and 9 (dotted) Gyr old Yonsei–Yale isochrones (Demarque et al. 2004) with $[\text{Fe}/\text{H}] = -0.35$ and $[\alpha/\text{Fe}] = 0.2$. We have also used a lighter gray color for the

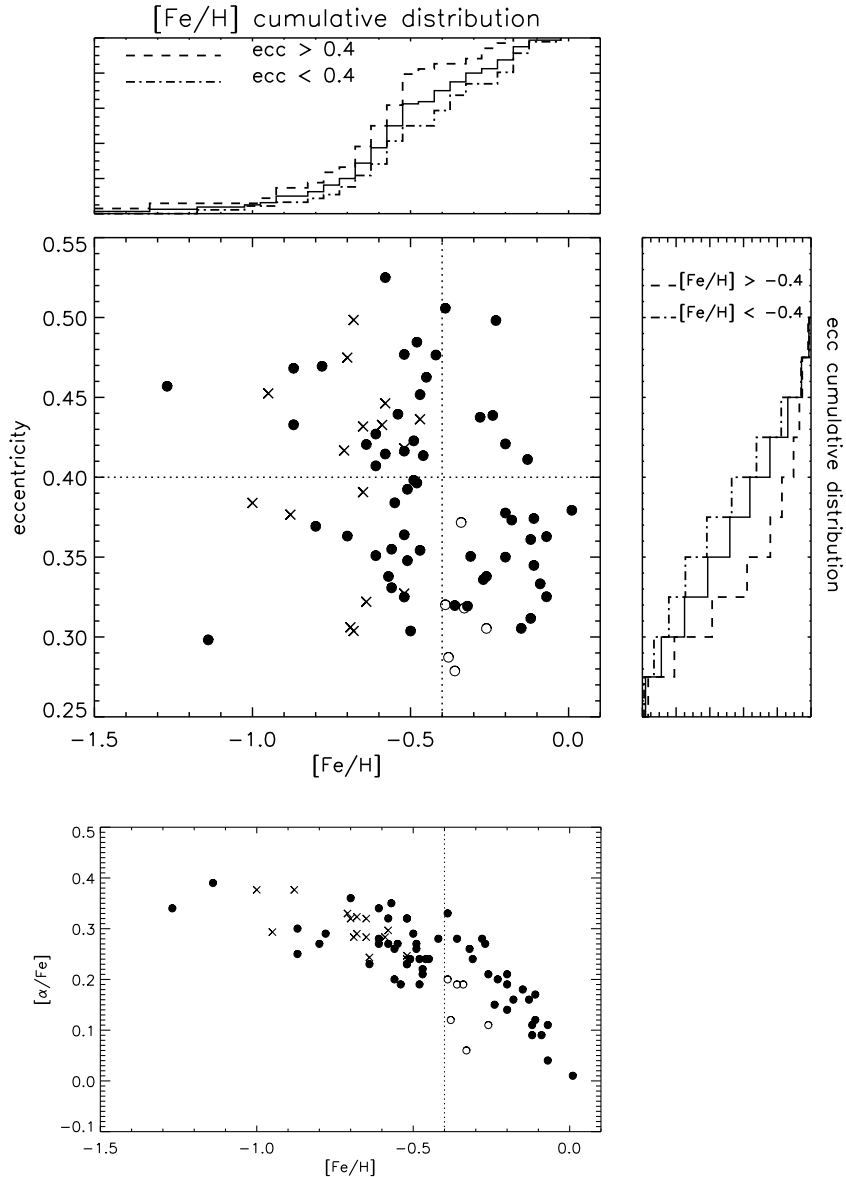


Figure 2. Eccentricity vs. $[\text{Fe}/\text{H}]$ (central panel), $[\alpha/\text{Fe}]$ vs. $[\text{Fe}/\text{H}]$ (bottom panel), and one-dimensional cumulative distributions of $[\text{Fe}/\text{H}]$ (top) and eccentricity (right) for stars in our sample (filled black circles) and those in ST (crosses). In the bottom panel we have indicated separately with open circles those stars possibly associated with a disrupted cluster. The lines at $[\text{Fe}/\text{H}] = -0.4$ and $\epsilon = 0.4$ indicate where a transition in populations seems to be present in our data set.

stars with $[\text{Fe}/\text{H}] > -0.4$ dex but higher $[\alpha/\text{Fe}]$. This allows the comparison of the age of the stars in the tentative cluster to those stars with similar metallicity and eccentricity. Clearly those “cluster” stars are on average younger (as they have bluer colors, higher temperatures), and consistent with being a single-age population. This motivates us to have a slight preference for the “cluster” scenario as it is not easy to understand why the contamination from the thin disk (which could be present for eccentricities ~ 0.3) would preferentially select stars with such a narrow range of $[\text{Fe}/\text{H}]$. Our sample has no bias against stars with high metallicities, so one would perhaps have expected contaminants from a broader range of $[\text{Fe}/\text{H}]$ to be more representative of the whole of the thin disk.

In summary, the bottom panel of Figure 2 shows that at high $[\text{Fe}/\text{H}]$, stars define a narrow sequence depicting a steep relation between $[\alpha/\text{Fe}]$ and $[\text{Fe}/\text{H}]$, and that a transition occurs at $[\text{Fe}/\text{H}] \sim -0.4$ dex, below which the scatter in $[\alpha/\text{Fe}]$ increases significantly. Therefore the joint analysis of the panels in Figure 2 suggests that at least two, but likely three, populations

co-exist in our data set: a low eccentricity population that dominates at high $[\text{Fe}/\text{H}]$, a high eccentricity population that is essentially only present at low $[\text{Fe}/\text{H}]$, and possibly a disrupted cluster. Note that none of these first two populations could belong to the thin disk given their kinematics and abundance trends. This is in agreement with the recent analysis of the *Gaia*-ESO survey by Recio-Blanco et al. (2014) that also shows a dearth of stars with high eccentricities at high $[\text{Fe}/\text{H}]$ in the thick disk.

Figure 4 shows various element ratios as a function of $[\text{Fe}/\text{H}]$ for all stars in our sample. We used the same symbol scheme as in the bottom panel of Figure 2, while the color coding (from dark to light) and symbol size (from small to large) indicate increasing values of eccentricity. The error bars correspond to two different estimates of our measurement uncertainties: from repeat observations of the same star (smaller bar) and from a global estimate⁶ (larger bar) derived from the change in the

⁶ Which is likely somewhat overestimated given the results from repeats.

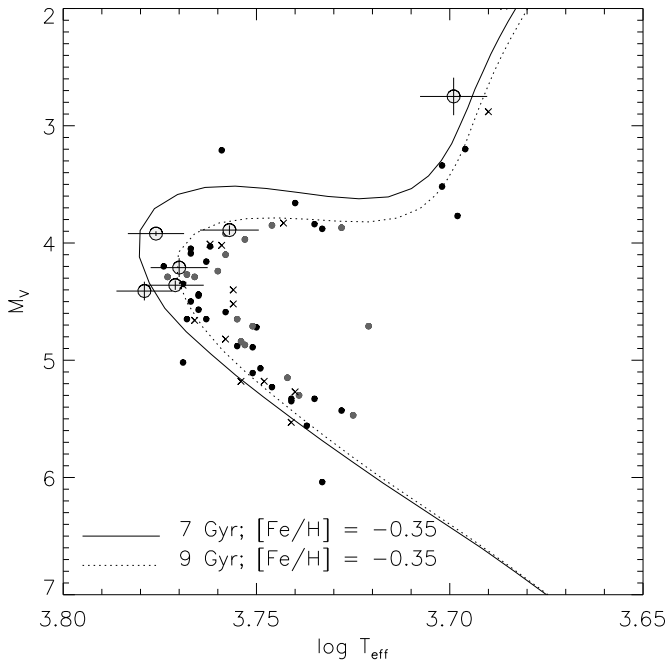


Figure 3. H-R diagram for the stars that we followed-up spectroscopically (solid symbols), and those from ST (crosses). Those in the tentative cluster identified in the bottom panel of Figure 2 are indicated with larger light gray symbols with error bars. Stars with $[\text{Fe}/\text{H}] > -0.4$ dex are shown in dark gray. The temperature error bars correspond to ± 100 K. The curves plotted are Yonsei–Yale isochrones (Demarque et al. 2004) with $[\text{Fe}/\text{H}] = -0.35$ and $[\alpha/\text{Fe}] = 0.2$.

abundance of a given element as T_{eff} varies by $\sim \pm 100$ K, $\log g$ by ± 0.1 , and $[\text{Fe}/\text{H}]$ by ± 0.1 . The black points in the panels correspond to stars from Reddy et al. (2003, 2006) that have $\epsilon < 0.3$ or $\epsilon > 0.5$ (to provide a comparison sample with different kinematical characteristics from the H06 set). To be on

the same scale, and using the 15 stars we have in common, we applied a zero-point correction $\Delta = [\text{E}/\text{H}]_{\text{us}} - [\text{E}/\text{H}]_{\text{Reddy}}$ to these abundances, namely, $\Delta[\text{Fe}/\text{H}] = 0.09$, $\Delta[\text{Mg}/\text{Fe}] = 0.06$, $\Delta[\text{Ca}/\text{Fe}] = 0.08$, $\Delta[\text{Ti}/\text{Fe}] = 0.01$, $\Delta[\text{Zn}/\text{Fe}] = 0.02$, $\Delta[\text{Cr}/\text{Fe}] = -0.03$, and $\Delta[\text{Ni}/\text{Fe}] = -0.03$ (for more details see Williams 2008). The stars in ST were first placed on the Reddy scale, and later shifted in the same way. The dashed lines in the $[\text{Mg}/\text{Fe}]$ versus $[\text{Fe}/\text{H}]$ panel correspond to the sequences for the thin and thick disks as determined by Fuhrmann (2011) in his volume-complete sample of nearby stars.

The three top left panels of this figure show that stars with $[\text{Fe}/\text{H}] > -0.4$ define a relatively narrow track in $[\text{Mg}/\text{Fe}]$, $[\text{Ca}/\text{Fe}]$, and $[\text{Ti}/\text{Fe}]$, with an internal dispersion smaller than the global estimated error, or even than the error determined from repeats. Note also that $[\text{Zn}/\text{Fe}]$ and even $[\text{Ni}/\text{Fe}]$ clearly follow distinct tracks as a function of $[\text{Fe}/\text{H}]$, despite the fact that both Zn and Ni are Fe-peak elements. Recall that in this region of chemical space most stars have lower eccentricities (darker symbols). We see once more that a transition in the chemical properties of the stars appears to occur at $[\text{Fe}/\text{H}] \sim -0.4$, as the scatter substantially increases for all elements below this metallicity (also in $[\text{SmII}/\text{Fe}]$, which is reasonable if this is largely an r -process product of massive stars, Mishenina et al. 2013). It is also interesting that the sequence delineated by the stars with $[\text{Fe}/\text{H}] > -0.4$ appears to define an upper envelope at lower $[\text{Fe}/\text{H}]$ (as there is a tendency for the darker symbols to have higher $[\alpha/\text{Fe}]$ at these lower metallicities, and perhaps also lower $[\text{SmII}/\text{Fe}]$). The higher eccentricity and more metal-poor stars (lighter colors and larger symbols) follow well the sequence of “thick” disk stars, and given their kinematics, could be part of the canonical thick disk (as suggested by, e.g., the uppermost dashed line in the $[\text{Mg}/\text{Fe}]$ versus $[\text{Fe}/\text{H}]$ panel).

Therefore the stars with lower ϵ tend to define the upper envelope of $[\alpha/\text{Fe}]$ versus $[\text{Fe}/\text{H}]$ both in our joint sample as

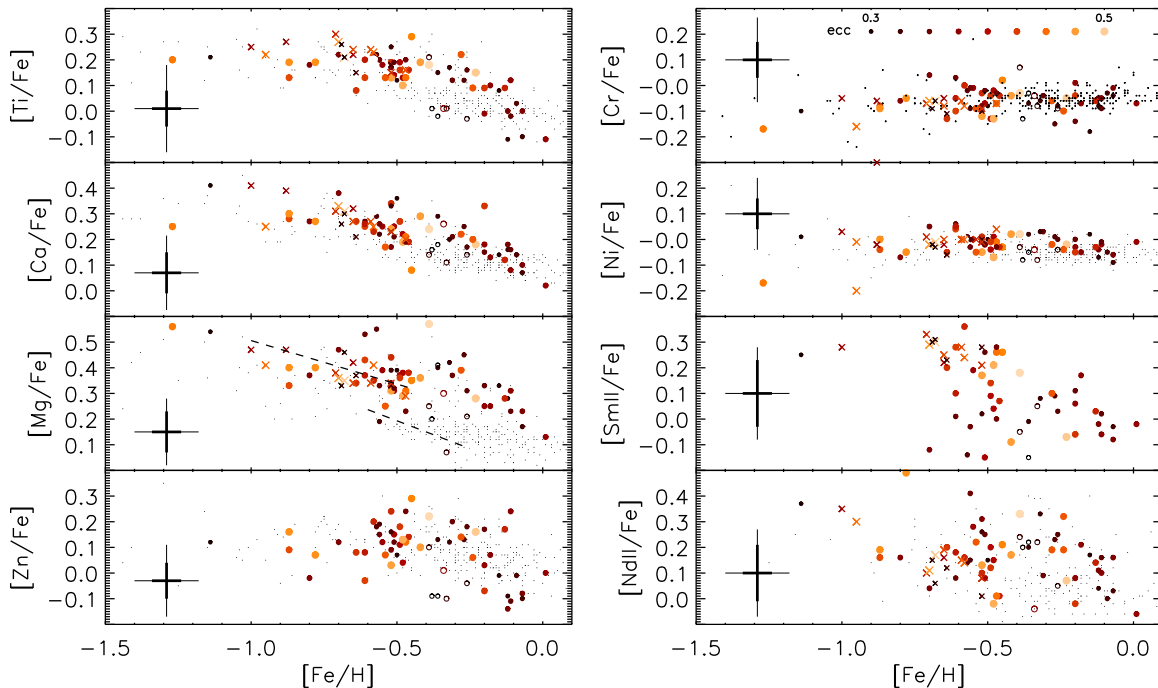


Figure 4. Various elements vs. $[\text{Fe}/\text{H}]$ for our sample of H06 stars (circles, where open symbols are for the tentative cluster) and for ST (crosses). The color-coding (dark to light) and symbol size (small to large) indicates increasing eccentricity as shown in the top right panel. For comparison, we also plotted (small dots) stars with $\epsilon < 0.3$ and $\epsilon > 0.5$ in the thin and thick disks from Reddy et al. (2003, 2006). The error bars indicate two estimates of our uncertainties: from repeats and from varying the derived astrophysical parameters.

(A color version of this figure is available in the online journal.)

well as in Reddy's. It is also interesting to note that the highest [Fe/H] stars have [Zn/Fe] and [Ti/Fe] lower than even the thin disk stars at this metallicity. On the other hand, their [Ca/Fe] is similar while their [Mg/Fe] is higher than even the thick disk stars at these [Fe/H].

The stars indicated with open symbols define very tight structures in [Ni/Fe] and also in [Ti/Fe]. In the other elements the scatter is consistent with the estimated global error. We may thus tentatively conclude that the indication of a single age (Figure 3), their location in abundance space (which overlaps generally with thin disk stars), and their tight kinematics all are consistent with a (star) cluster origin for these stars.

The two stars with [Fe/H] ~ -0.87 (HD 25704 and HD 63598) are particularly intriguing since they have nearly identical compositions in all elements. They also share the same location in the H-R diagram, implying that they have the same age (also confirmed by Casagrande et al. 2011). Furthermore, their distances are essentially identical (~ 50 pc). According to their kinematics, they would be on relatively eccentric orbits, with $\epsilon = 0.43$ and 0.47 and velocities $(U, V, W) = (-127, -67, -9)$ km s $^{-1}$ and $(16, -108, 1)$ km s $^{-1}$, with average errors of 3 and 2 km s $^{-1}$ respectively. A possibility is that these stars constitute a binary, as their velocity difference is too large for them to be located on the same orbital phase as a tidal stream.

3. DISCUSSION

We have shown that stars with $0.3 \leq \epsilon \leq 0.5$ do not form a homogeneous population. In this eccentricity range, a few populations with different characteristics are found.

1. High metallicity stars ([Fe/H] > -0.4 dex) predominantly have lower eccentricities ($\epsilon \leq 0.4$), cold vertical kinematics, are $[\alpha/\text{Fe}]$ enhanced, and define a relatively narrow track in all α elements versus [Fe/H], as well as in Zn and Ni. While their kinematics might suggest they could constitute the tail of the thin disk population, their abundances clearly rule out this possibility. This population is dominated by stars with an average age of 8 Gyr, and has no stars older than 12 Gyr.
2. Lower metallicity stars can be on high or low eccentricity orbits, and show a larger abundance scatter than the population described in the previous item, and are also on average older, i.e., ~ 9 Gyr, with several stars as old as 14 Gyr. The higher eccentricity stars could be considered representative of the canonical thick disk.
3. The third group of stars present in our data set have very similar iron-peak abundances and a somewhat larger scatter in α elements, especially in [Mg/Fe]. Half of these stars are also kinematically clustered in a tight clump, and all have similarly low eccentricities and ages, suggesting that they form a dynamical entity with a scale perhaps similar to that of a (star) cluster.

It is interesting to note that the first population overlaps with the high α metal-rich population in Adibekyan et al. (2013; who also miss high-eccentricity metal-rich stars; see their Figure 5). However, in our sample, as in Bensby et al. (2014), there is no gap in [Fe/H] between this population and the more metal-poor stars.

The issue now is how to interpret these two main populations (i.e., excluding the tentative cluster) in the context of the evolution of our Galaxy. Let us consider the following possibilities.

1. *Mergers.* In the most widely discussed scenario for the formation of the thick disk, a pre-existing disk is heated up

via a minor merger. Such a disk would be more massive and hence have a higher metallicity and lower eccentricity than the accreted population (Sales et al. 2009). Thus we would be tempted to identify this population with the sequence defined by the more metal-rich stars in our data set, and the intruder with the higher eccentricity and lower [Fe/H] stars. The colder kinematics of the first group, ages and enhanced $[\alpha/\text{Fe}]$ (i.e., higher star formation rate indicating more massive) would also seem to support this view.

2. *Canonical Thick Disk and Bulge.* Stars with higher eccentricities could be associated with the canonical thick disk, while those that are more metal-rich could on the basis of their abundance patterns and ages be the extension of the bulge to the solar neighborhood. If this scenario is enforced, it would seem to be necessary to argue that the bulge/bar stars' eccentricities and vertical motions are on average lower than those of the canonical thick disk, which appears slightly counterintuitive given our knowledge of in situ bulge stars (e.g., Soto et al. 2012).
3. *Radial Migration.* In this scenario the high metallicity population would originate from the inner galactic disk (Grenon 1999; Schoenrich & Binney 2009). Hence one might expect such stars to have higher eccentricities (although migrated stars can also be on nearly circular orbits) as well as hotter σ_z on average as postulated by Schoenrich & Binney (2009; although see Minchev et al. 2012, who argue that if the vertical action is conserved, then the stars migrating from the inner disk become colder). On the other hand, the population of low [Fe/H] could not be considered the migrated population from the outer disk (as in the model by Haywood 2008), because its σ_z is higher than that of the thin disk locally, contrary to the prediction from simulations including radial migration (e.g., Solway et al. 2012; Minchev et al. 2012).

Which of these three scenarios is more likely is unclear, although the last one appears less plausible at face value when accounting for all the features observed.

It is interesting that we have not found that stars cluster in tight lumps at a fixed metallicity, except in a few occasions. Rather, we found sequences as expected for populations that have had a finite time to evolve (and self-enrich). The chemical evolution tracks are probably indicative of fairly intense star formation histories, rather unlike those of, e.g., dSph.

Our work suggests that the Milky Way's disk(s) is (are) the overlap of several populations with distinct characteristics. The combination of dynamics, stellar population analysis, and chemical abundances have allowed us to establish this. However, we seem to be still a long way from being able to deconstruct and understand the history of the Milky Way.

We thank Peter Stetson for his DAOSPEC code used in the equivalent width analysis. We thank Jon Fulbright for providing a model-atmosphere interpolation code, with the kind permission of Jennifer Johnson. A.H. was partially supported by ERC-StG GALACTICA-240271 and NWO-VIDI grants. This research made use of the Vienna Atomic Line Database, Austria, the SIMBAD database at CDS, France, and the NASA ADS, USA.

REFERENCES

- Abadi, M. G., Navarro, J. F., Steinmetz, M., & Eke, V. R. 2003, *ApJ*, 591, 499
 Adibekyan, V. Z., Figueira, P., Santos, N. C., et al. 2013, *A&A*, 554, A44

- Arifyanto, M. I., & Fuchs, B. 2006, *A&A*, **449**, 533
- Arlandini, C., Käppeler, F., Wisshak, K., et al. 1999, *ApJ*, **525**, 886
- Belokurov, V., Zucker, D. B., Evans, N. W., et al. 2006, *ApJL*, **642**, L137
- Bensby, T., Feltzing, S., & Lundström, I. 2003, *A&A*, **410**, 527
- Bensby, T., Feltzing, S., Lundström, I., & Ilyin, I. 2005, *A&A*, **433**, 185
- Bensby, T., Feltzing, S., & Oey, M. S. 2014, *A&A*, 526, A71
- Bullock, J. S., & Johnston, K. V. 2005, *ApJ*, **635**, 931
- Burris, D. L., Pilachowski, C. A., Armandroff, T. E., et al. 2000, *ApJ*, **544**, 302
- Casagrande, L., Schönrich, R., Asplund, M., et al. 2011, *A&A*, **530**, A138
- De Silva, G. M., Freeman, K. C., Bland-Hawthorn, J., Asplund, M., & Bessell, M. S. 2007, *AJ*, **133**, 694
- Demarque, P., Woo, J. H., Kim, Y. C., & Yi, S. 2004, *ApJS*, **155**, 667
- Freeman, K. C., & Bland-Hawthorn, J. 2002, *ARA&A*, **40**, 487
- Fuhrmann, K. 2011, *MNRAS*, **414**, 2893
- Gilmore, G., Wyse, R. F. G., & Norris, J. E. 2002, *ApJL*, **574**, L39
- Grenon, M. 1999, *Ap&SS*, **265**, 331
- Haywood, M. 2008, *MNRAS*, **388**, 1175
- Helmi, A., Navarro, J. F., Nordström, B., et al. 2006, *MNRAS*, **365**, 1309
- Helmi, A., & White, S. D. M. 1999, *MNRAS*, **307**, 495
- Helmi, A., White, S. D. M., de Zeeuw, P. T., & Zhao, H. 1999, *Natur*, **402**, 53
- Holmberg, J., Nordström, B., & Andersen, J. 2009, *A&A*, **501**, 941
- Majewski, S. R., Nidever, D. L., Smith, V. V., et al. 2012, *ApJL*, **747**, L37
- Meza, A., Navarro, J. F., Abadi, M. G., & Steinmetz, M. 2005, *MNRAS*, **359**, 93
- Minchev, I., Famaey, B., Quillen, A. C., et al. 2012, *A&A*, **548**, A127
- Mishenina, T. V., Pignatari, M., Korotin, S. A., et al. 2013, *A&A*, **552**, A128
- Navarro, J. F., Helmi, A., & Freeman, K. C. 2004, *ApJL*, **601**, L43
- Newberg, H. J., Yanny, B., Rockosi, C., et al. 2002, *ApJ*, **569**, 245
- Nissen, P. E., & Schuster, W. J. 2010, *A&A*, **511**, L10
- Nissen, P. E., & Schuster, W. J. 2011, *A&A*, **530**, A15
- Nordström, B., Mayor, M., Anderson, J., et al. 2004, *A&A*, 418, 989
- Recio-Blanco, A., de Laverny, P., Kordopatis, G., et al. 2014, *A&A*, 567, A5
- Reddy, B. E., Lambert, D. L., & Allende Prieto, C. 2006, *MNRAS*, **367**, 1329
- Reddy, B. E., Tomkin, J., Lambert, D. L., & Allende Prieto, C. 2003, *MNRAS*, **340**, 304
- Richardson, J. C., Ferguson, A. M. N., Johnson, A., et al. 2008, *AJ*, **135**, 1998
- Sales, L. V., Helmi, A., Abadi, M. G., et al. 2009, *MNRAS*, **400**, L61
- Schönrich, R., & Binney, J. 2009, *MNRAS*, **399**, 1145
- Snedden, C. 1973, PhD thesis, Univ. Texas, Austin
- Solway, M., Sellwood, J. A., & Schönrich, R. 2012, *MNRAS*, **422**, 1363
- Soto, M., Kuijken, K., & Rich, R. M. 2012, *A&A*, **540**, A48
- Stetson, P. B., & Pancino, E. 2008, *PASP*, **120**, 1332
- Stonkutė, E., Tautvaišė, G., Nordström, B., & Ženovienė, R. 2012, *A&A*, **541**, A157
- Stonkutė, E., Tautvaišė, G., Nordström, B., & Ženovienė, R. 2013, *A&A*, **555**, A6
- Williams, M. E. K. 2008, PhD thesis, Australian National Univ.
- Yllie-de Boer, E., Freeman, K., & Williams, M. 2010, *AJ*, **139**, 636
- Yllie-de Boer, E., Freeman, K., Williams, M., et al. 2012, *ApJ*, **755**, 35